J. Biochem. 2016;159(2):225–237 doi:10.1093/jb/mvv098

JB THE JOURNAL OF BIOCHEMISTRY

Intracellular accumulation of indium ions released from nanoparticles induces oxidative stress, proinflammatory response and DNA damage

Received August 3, 2015; accepted August 19, 2015; published online September 15, 2015

Yosuke Tabei*, Akinari Sonoda, Yoshihiro Nakajima, Vasudevanpillai Biju, Yoji Makita, Yasukazu Yoshida and Masanori Horie

Health Research Institute, National Institute of Advanced Industrial Science and Technology, 2217-14 Hayashi-cho, Takamatsu, Kagawa 761-0395, Japan

*Yosuke Tabei, Health Research Institute, National Institute of Advanced Industrial Science and Technology, 2217-14 Hayashi-cho, Takamatsu, Kagawa 761-0395, Japan. Tel: +81-87-869-3598, Fax: +81-87-869-3553, email: y-tabei@aist.go.jp

Due to the widespread use of indium tin oxide (ITO), it is important to investigate its effect on human health. In this study, we evaluated the cellular effects of ITO nanoparticles (NPs), indium chloride ($InCl_3$) and tin chloride ($SnCl_3$) using human lung epithelial A549 cells. Transmission electron microscopy and inductively coupled plasma mass spectrometry were employed to study cellular ITO NP uptake. Interestingly, greater uptake of ITO NPs was observed, as compared with soluble salts. ITO NP species released could be divided into two types: 'indium release ITO' or 'tin release ITO'. We incubated A549 cells with indium release ITO, tin release ITO, $InCl_3$ or $SnCl_2$ and investigated oxidative stress, proinflammatory response, cytotoxicity and DNA damage. We found that intracellular reactive oxygen species were increased in cells incubated with indium release ITO, but not tin release ITO, $InCl_3$ or $SnCl_2$. Messenger RNA and protein levels of the inflammatory marker, interleukin-8, also increased following exposure to indium release ITO. Furthermore, the alkaline comet assay revealed that intracellular accumulation of indium ions induced DNA damage. Our results demonstrate that the accumulation of ionic indium, but not ionic tin, from ITO NPs in the intracellular matrix has extensive cellular effects.

Keywords: DNA damage/indium tin oxide/nanoparticles/oxidative stress/proinflammatory response.

Abbreviations: cDNA, complementary DNA; DCFH-DA, 2′,7′-dichlorodihydrofluorescin diacetate; DLS, dynamic light scattering; DMEM, Dulbecco's modified Eagle's medium; FBS, fetal bovine serum; FE-SEM, field emission scanning electron microscopy; HMOX-1, heme oxygenase 1; ICP-AES, inductively coupled plasma atomic emission spectrometry; ICP-MS, ICP-mass spectrometry; IL-8, interleukin-8; ITO, indium tin oxide; LDH, lactate dehydrogenase; mRNA, messenger RNA; MTIIA, metallothionein IIA; NP, nanoparticle; PCR, polymerase chain reaction; ROS, reactive oxygen species; TEM, transmission electron microscopy.

A nanoparticle (NP) is a particle with a diameter between 1 and 100 nm (ISO/TS 27678:2008). NPs have unique physicochemical properties, including high catalytic activity and distinct absorption spectra, as compared with micro-sized particles (*1*). These unique properties are beneficial for industrial use, and many NPs are used in consumer products, such as sunscreen, cosmetics and food additives. Additionally, several studies have focused on clinical applications of NPs, including nanomedicine and drug-delivery systems (*2*, *3*). However, despite these potential advantages, NPs also induce several biological effects. For example, zinc oxide (ZnO) NPs are used in industrial materials, such as electronic components and sunscreen. However, several *in vitro* and *in vivo* studies have revealed severe cytotoxic effects following ZnO NP administration (*4*–*7*). Therefore, precise, case-by-case evaluation of NP-mediated cellular effects is required to avoid both the negative health effects and unnecessary prohibition of NPs.

The chemical composition of metal and metal oxide NPs is an important factor when considering cellular effects. For example, ZnO, copper oxide (CuO), nickel oxide (NiO) and antimony oxide NPs exert strong cytotoxicity, whereas titanium dioxide, cerium oxide and aluminum oxide NPs have weak cellular effects (*8*). Additionally, the metal ions released from NPs are an important parameter in the evaluation of the cellular effects of NPs (*9*). For example, ZnO, NiO and chromium oxide NPs solubilized in cell culture medium release the corresponding metal ions into the extracellular environment, exerting remarkable cytotoxicity (*7*, *10*, *11*). Internalized metal and metal oxide NPs continuously release metal ions, leading to metabolic dysfunction. For example, the cytotoxic effects of silver (Ag) and CuO NPs are mediated by cellular uptake and intracellular release of Ag and copper ions (*12*, *13*). Therefore, to understand the mechanisms underlying NP-mediated cellular effects, the material properties, including cellular uptake and intracellular behaviour, must be considered.

In this study, we evaluated the cellular effects of indium tin oxide (ITO) NPs. ITO is a sintered material consisting of indium oxide (In_2O_3; typically 90%) and tin oxide (SnO_2; typically 10%). This material is widely used as a transparent conducting electrode in various

photoelectron devices, including liquid crystal displays and solar panels (*14*, *15*), and is also used in protein microarrays and gas sensing devices (*16*, *17*). The preparation and property control of nano-sized ITO particles is of interest because of their potential beneficial applications in versatile devices (*18*, *19*). Due to the wide-spread applications of ITO, it is important to investigate their possible effects on human health. The genotoxic effects of indium and tin-containing compounds were previously reported (*20*, *21*). Recently, Badding *et al*. (*22*) demonstrated that ITO induced robust cytokine production in both mouse macrophages and human bronchial epithelial cells. Additionally, occupational exposure in an ITO worker resulted in severe interstitial pneumonia and death due to bilateral pneumothorax in Japan (*23*). Furthermore, epidemiological studies and studies of fatal cases in workers exposed to ITO show that ITO induces occupational lung disease and is associated with a risk of interstitial lung damage (*24–27*). However, it remains unclear whether inhalation of ITO is a potential occupational health hazard in employees handling these materials.

The aim of this study was to investigate ITO NP-mediated cellular effects using human lung epithelial A549 cells. A549 cells are well-characterized *in vitro* model for investigating molecular and biochemical processes in airway epithelium, and are widely regarded as a valid model system for NP-induced pulmonary effects. Recently, we demonstrated that the ITO NPs possess the potential for inducing oxidative stress and DNA damage in the A549 cells (*28*); however, possible differences in cellular effects between ITO NPs and their corresponding metal ionic species have not been assessed yet. In this study, we focused on the importance of ITO NP cellular uptake and the subsequent release of metal ions inside the cell. Furthermore, we compared the cellular effects of ITO NPs and their corresponding metal ionic species, and examined the mechanisms underlying these effects.

Experimental Procedure

Preparation of stable ITO dispersions

ITO NPs were purchased from C. I. Kasei Co., Ltd (Tokyo, Japan) and Tomoe Works Co., Ltd (Hyogo, Japan). Physical characteristics of the ITO NPs are reported in Table I. The surface area of ITO NPs which were degassed at 120°C for 30 min was determined using a Quantachrom Autosorb-1 instrument using nitrogen adsorption and the five-point Brunauer–Emmett–Teller method. Stable ITO dispersions were prepared as described previously (*28*). In brief, ITO NPs were dispersed in 1% bovine serum albumin at a concentration of 80 mg/ml by sonication. Subsequently, the dispersions were centrifuged at $4{,}000 \times g$ for 20 min. Precipitated ITO NPs were re-dispersed in an equivalent volume of fresh culture medium. The dispersions were centrifuged at $1{,}000 \times g$ for 20 min. For Sample A, the resultant $1{,}000 \times g$ fraction was used for cellular response examination. Because the $1{,}000 \times g$ fraction of Sample B did not contain sufficient ITO NPs, the centrifugal force was reduced from $1{,}000 \times g$ to $500 \times g$.

Characterization of stable ITO dispersions

Observation of the ITO NP microstructure in stable ITO dispersions was carried out using field emission scanning electron microscopy (FE-SEM, JSM-6700F; JOEL Ltd, Tokyo, Japan). T secondary particle size of the ITO NPs in the stable ITO dispersions was determined using a Dynamic Light Scattering (DLS) Particle Size Analyzer (LB-550; HORIBA Ltd, Kyoto, Japan) at 25.0°C ± 0.1°C. The light source was a 650-nm laser diode of 5 mW. Approximately 20-ml aqueous ITO dispersion was measured directly without any pre-treatment.

The concentrations of In_2O_3 and SnO_2 included in the stable ITO dispersions were measured by inductively coupled plasma atomic emission spectrometry (ICP-AES; Thermo Jarrell Ash Corp., Franklin, MA) and ICP-mass spectrometry (ICP-MS; X-Series II; ThermoFischer Scientific, Inc., Waltham, MA). To determine the concentration of medium components, stable ITO dispersions were collected through ultrafiltration membranes (Amicon Ultra Centrifugal Filters Ultracel 30K; Merck Millipore, Billerica, MA) and centrifuged at $7{,}000 \times g$ for 20 min. The concentrations of In, Sn, Na, Ca and P were determined by ICP-AES (SPS7800; Seiko Instruments, Inc., Tokyo, Japan) and ICP-MS.

Cell culture and treatment

Human lung epithelial A549 cells (RCB0098) were purchased from RIKEN BioResource Center (Ibaraki, Japan). Cells were cultured in Dulbecco's modified Eagle's medium (DMEM; Gibco Life Technologies, Gaithersburg, MD) supplemented with 10% heat-inactivated fetal bovine serum (FBS; USDA Tested FBS; ThermoFischer Scientific, Inc.), 100 U/ml penicillin, 100 µg/ml streptomycin and 250 ng/ml amphotericin B (Nacalai Tesque, Inc., Kyoto, Japan). This DMEM preparation is referred to as 'DMEM-FBS'. Cells in DMEM-FBS were placed in 80 cm^2 flasks (ThermoFischer Scientific, Inc.) and cultured at 37°C in an atmosphere containing 5% CO_2. For experiments, cells were seeded in different size multi-well plates (ThermoFischer Scientific, Inc.) at a density of 1×10^5 cells/ml and incubated for 24 h. Subsequently, culture medium was replaced by DMEM-FBS supplemented with the stable ITO dispersion, $InCl_3$ or $SnCl_2$ solution (Wako Pure Chemical Ind., Osaka, Japan) and incubated at 37°C in an atmosphere of 5% CO_2.

Transmission electron microscopy observation

A549 cells exposed to stable ITO dispersions for 24 h were fixed using 1.2% glutaraldehyde (TAAB Laboratories Equipment Ltd, Aldermaston, UK) for 1 h. The fixed samples were treated with OsO_4 solution for 1 h, dehydrated in ethanol and embedded in epoxy resin. The resultant samples were cut into ultrathin sections suitable for transmission electron microscopy (TEM) observation by diamond-knife ultramicrotomy. TEM observation was then carried out using H-7600 (Hitachi Corp., Tokyo, Japan). The acceleration voltage was 80 kV.

Table I. ITO sample characteristics

	Primary particle size (nm)		Specific surface area (m^2/g)	
Names in this study	Manufacturer's data[a]	FE-SEM (in stable dispersion)	Manufacturer's data[a]	Five-point Brunauer–Emmett–Teller method
Sample A	26	8–50 (average = 20.8)	35	30.8
Sample B	25.1	7–20 (average = 12.0)	n/a	34.7

[a]According to the manufacturer's data sheet. Other data were measured in this study.
n/a = not available.

Cellular uptake of ITO NPs

The delivery of ITO NPs to the cell surface and intracellular space was measured using ICP-MS. A549 cells were exposed to stable ITO dispersions for 24 h, washed with phosphate buffered saline (PBS) three times to remove loosely bound ITO NPs on the cell surface and detached by trypsinization (0.25%). The cell pellet was suspended in 1 ml PBS, and the number of cells was counted using a hemocytometer. The cells were mixed with acidic solution (water:nitric acid:hydrochloric acid = 4:1:3) and then heated at 80°C for 2 h to dissolve the cellular content. The dissolved solutions were diluted with water and used for ICP-MS measurement.

Isolation of total RNA and quantitative real-time polymerase chain reaction

Cells were cultured in 6-well plates and incubated in the stable ITO dispersions, $InCl_3$ or $SnCl_2$ solutions for 24 h. Subsequently, total RNA was extracted using the RNeasy mini kit (Qiagen, Valencia, CA) according to manufacturer's instructions. The total RNA concentrations were determined using a Nanodrop ND-1000 spectrophotometer (ThermoFischer Scientific, Inc.). First strand complementary DNA (cDNA) was synthesized from 0.5 μg total RNA using the SuperScript VILO cDNA synthesis kit (Invitrogen, Carlsbad, CA) according to the manufacturer's instructions. The messenger RNA (mRNA) levels of metallothionein IIA (*MTIIA*), heme oxygenase 1 (*HMOX-1*) and interleukin-8 (*IL-8*) were analysed using the TaqMan gene expression assay (IDs: MTIIA, Hs02379661_g1; HO-1, Hs01110250_m1; IL-8, Hs00174103_m1; Applied Biosystems, Foster City, CA). The housekeeping gene β-actin (ID: Hs99999903_m1) was used as an internal control. Target mRNA levels were measured using an Applied Biosystems 7300 real-time polymerase chain reaction (PCR) system. The cycler conditions were as follows: 2 min at 50°C, 10 min at 95°C and 60 cycles each of 15 s at 95°C and 1 min at 60°C. The mRNA expression levels of *MTIIA*, *HMOX-1* and *IL-8* in each sample were normalized to β-actin, and were then compared with untreated controls. The results are reported as fold change over control.

IL-8 enzyme-linked immunosorbent assay

Cells were cultured in 6-well plates and incubated in the stable ITO dispersions, $InCl_3$ or $SnCl_2$ solutions for 24 h. Subsequently, IL-8 protein levels in the culture supernatants were measured using an enzyme-linked immunosorbent assay kit (eBioscience, San Diego, CA) following the manufacturer's instruction.

Measurement of intracellular reactive oxygen species levels

Intracellular reactive oxygen species (ROS) were detected using 2′,7′-dichlorodihydrofluorescin diacetate (DCFH-DA) (Sigma-Aldrich, St. Louis, MO). After incubating the cells with stable ITO dispersions, $InCl_3$ or $SnCl_2$ solution, the medium was changed to serum-free DMEM containing 10 μM DCFH-DA. Cells were incubated for 30 min at 37°C, washed once with PBS, collected by trypsinization (0.25%), washed again with PBS and resuspended in 500 μl PBS. Cell samples in PBS were excited with a 488-nm argon ion laser in a FACSCalibur flow cytometer (Becton, Dickinson and Company, Franklin Lakes, NJ). The DCF emission was recorded at 525 nm. Data were collected from at least 5,000 gated events.

Water-soluble tetrazolium salts-1 (WST-1) assay

Cell viability was examined using WST-1 solution (Premix WST-1 Cell Proliferation Assay System; Takara Bio, Shiga, Japan). Cells were cultured in 96-well plates and incubated in the stable ITO dispersions, $InCl_3$ or $SnCl_2$ solutions for 24 h. To determine cell viability, the cells were incubated with 10-fold diluted WST-1 solution at 37°C for 1 h. The optical density of formazan was measured at 450 nm using Tecan Infinite M200 (Tecan Group Ltd, Männedorf, Switzerland).

Lactate dehydrogenase assay

Cells were cultured in 12-well plates and incubated in the stable ITO dispersions, $InCl_3$ or $SnCl_2$ solutions for 24 h. Lactate dehydrogenase (LDH) release was measured using the Cytotoxicity Detection Kit^{PLUS} (LDH) (Roche Diagnostics GmbH, Mannheim, Germany) according to the manufacturer's protocol. The cytotoxicity was calculated as follows: cytotoxicity (%) = (experimental value − low control)/(high control − low control) × 100. The low control, which refers to spontaneous LDH release, was the LDH released from untreated normal cells. The high control, which refers to the maximum LDH release, was the LDH released from cells that were lysed using the lysis solution provided in the kit.

Alkaline comet assay

An alkaline comet assay was performed according to the instructions provided by the manufacturer (Comet Assay; Trevigen, Gaithersburg, MD). Cells (2×10^5 cells/ml) were seeded in 6-well plates. After overnight incubation, the cells were exposed to the stable ITO dispersions, $InCl_3$ or $SnCl_2$ solutions for 24 h. Cells were then washed and resuspended in Ca^{2+}- and Mg^{2+}-free PBS solution. The cell suspension (1×10^5 cells/ml) was mixed with LMagarose at a ratio of 1:10 (v/v). This mixture was immediately transferred onto the CometSlide (Trevigen). After cell lysis at 4°C, CometSlides were treated with an alkaline unwinding solution (0.2 M NaOH and 1 mM ethylenediaminetetraacetic acid, pH > 13) for 60 min. The CometSlides were placed on a horizontal electrophoresis unit and the unit was filled with fresh buffer alkaline unwinding solution until the CometSlides were covered. Electrophoresis was performed at 20 V for 35 min at 4°C in the dark, and then staining was performed with an Ag-staining kit (Trevigen). The comet tail length was defined as the distance between the leading edge of the nucleus and the end of the tail. At least 50 determinations were performed for each sample.

Clonogenic assay

Colony-forming ability was detected using a clonogenic assay based on methods described by Herzog *et al.* (*29*) and Franken *et al* (*30*). Briefly, the cells were seeded in 6-well plates (300 cells/well) and allowed to attach for 20 h. Cells were then treated with the stable ITO dispersions, $InCl_3$ or $SnCl_2$ solutions and cultured until control cells formed colonies (one colony was defined as ≤50 cells, 7 days). Subsequently, the dispersions were removed and the cells were washed with 2 ml PBS. After fixation with 100% methanol for 20 min, the cells were stained with Giemsa's staining solution (Kanto Chemical Co., Inc., Tokyo, Japan) for 20 min and rinsed with distilled water. The number of colonies was counted.

Statistical analysis

Data present the mean ± standard deviation from at least three independent experiments. Statistical analyses were performed by the analysis of variance using the Dunnett test for multiple comparisons.

Results and Discussion

Preparation and characterization of stable ITO dispersions

To investigate the cellular effect of NPs, the preparation of a stable NP-medium dispersion was necessary (*31*). When ITO NPs were dispersed in DMEM-FBS, ITO NPs formed large secondary particles and sedimented within a few minutes by gravity. Therefore, we prepared stable ITO dispersions by pre-adsorption and centrifugal fractionation methods as reported previously (*28*). The results of the ITO dispersion characterization are summarized in Table II. The concentrations of In_2O_3 in the ITO dispersions of Sample A and Sample B were 720 and 200 μg/ml, respectively. The concentrations of SnO_2 in Sample A and Sample B were 70 and 15 μg/ml, respectively. FE-SEM observations revealed that the ITO NPs in the prepared dispersions were globular particles (Fig. 1A). The primary particle sizes in Sample A and Sample B were within the ranges of 8–50 and 7–20 nm, respectively (Table I). Sample A contained non-uniform ITO NPs and had a broad distribution of primary particle sizes. In contrast, Sample B

Table II. Characterization of the ITO–DMEM–FBS dispersions used in this study

	Metal oxide concentration (μg/ml)		Metal concentration in the filtrate (μM)		Salt composition of the dispersion		
Names in this study	In_2O_3	SnO_2	In	Sn	Na (mM)	Ca (mM)	P (μM)
Sample A	720	70	0.03	0.37	145	0.8	87
Sample B	200	15	0.25	0.08	150	1.5	53
DMEM-FBS			0.02	0.00	170	1.9	66

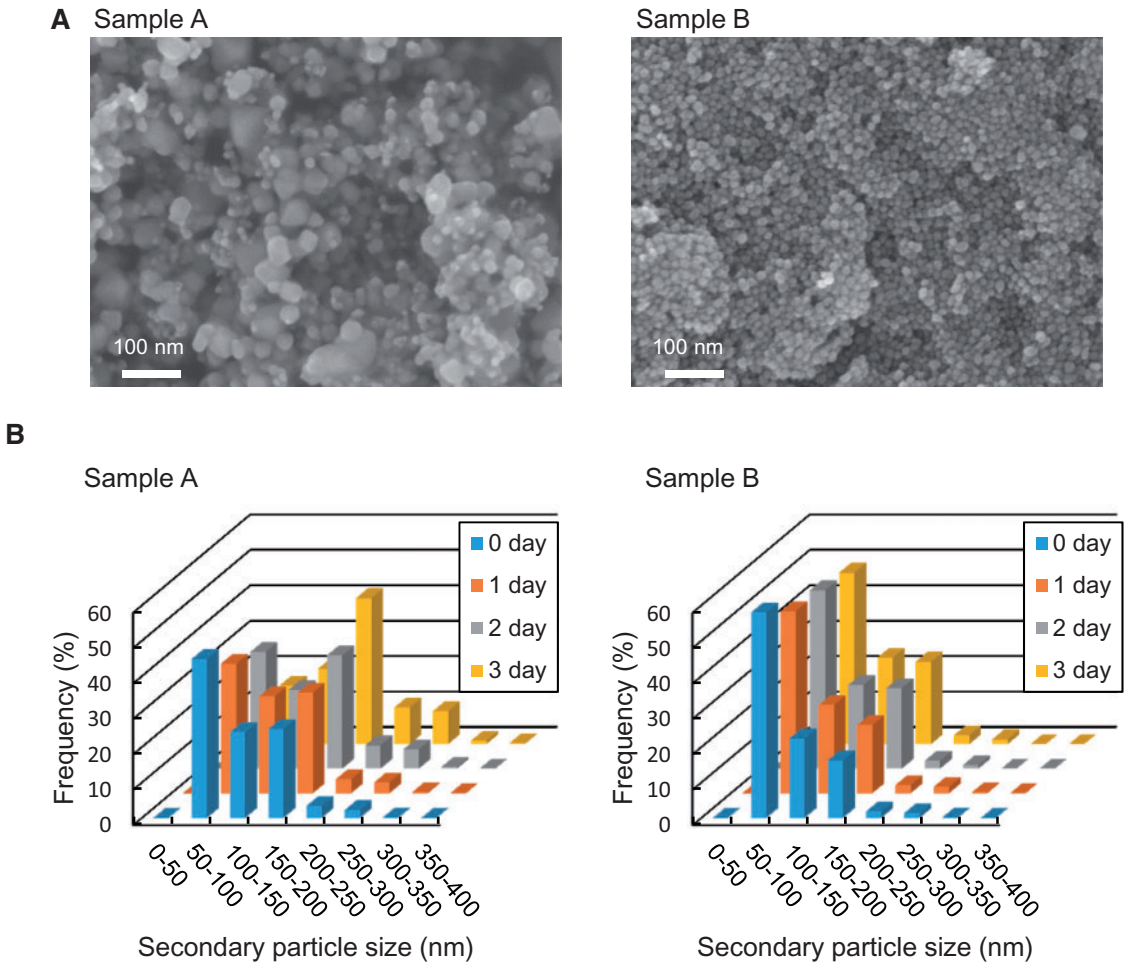

Fig. 1 Size distributions of ITO NPs in stable ITO dispersions. (**A**) FE-SEM analysis of ITO NPs included in stable ITO dispersions. (**B**) Histogram of secondary ITO NP sizes based on particle number measured by DLS. The stable ITO dispersions were prepared on day 0.

contained uniform ITO NPs and had a narrow particle size distribution.

Previous studies showed that dispersion stability is important to evaluate the cellular effects of NPs (*32*, *33*). The stability of the ITO dispersions was evaluated by DLS measurement. After 3 days, the relative light scattering intensities of Sample A and Sample B were decreased to 88% and 92%, respectively, indicating that gravity sedimentation was not remarkable. The secondary particle size of ITO NPs in the dispersion was also measured by DLS (Fig. 1B). The secondary particle size histogram of Sample A revealed secondary particle sizes between 50 and 100 nm after preparation (at 0 day), which gradually increased over 3 days. However, the secondary particle size of Sample B did not change during the experimental period. These results indicate that, although slight aggregation was observed in Sample A, both ITO dispersions prepared in this study were stable for 3 days and suitable for cellular experiments.

Cellular uptake of ITO NPs by A549 cells

Cellular uptake is an important process that governs the effects of NPs. To investigate the uptake and intracellular localization of ITO NPs, we performed ultrastructure analysis with TEM (Fig. 2A). TEM images clearly showed the incorporation of ITO NPs into A549 cells after 24-h incubation. The ITO NPs were observed in cellular compartments, primarily in lysosome-like structures. Other cellular organelles, such as

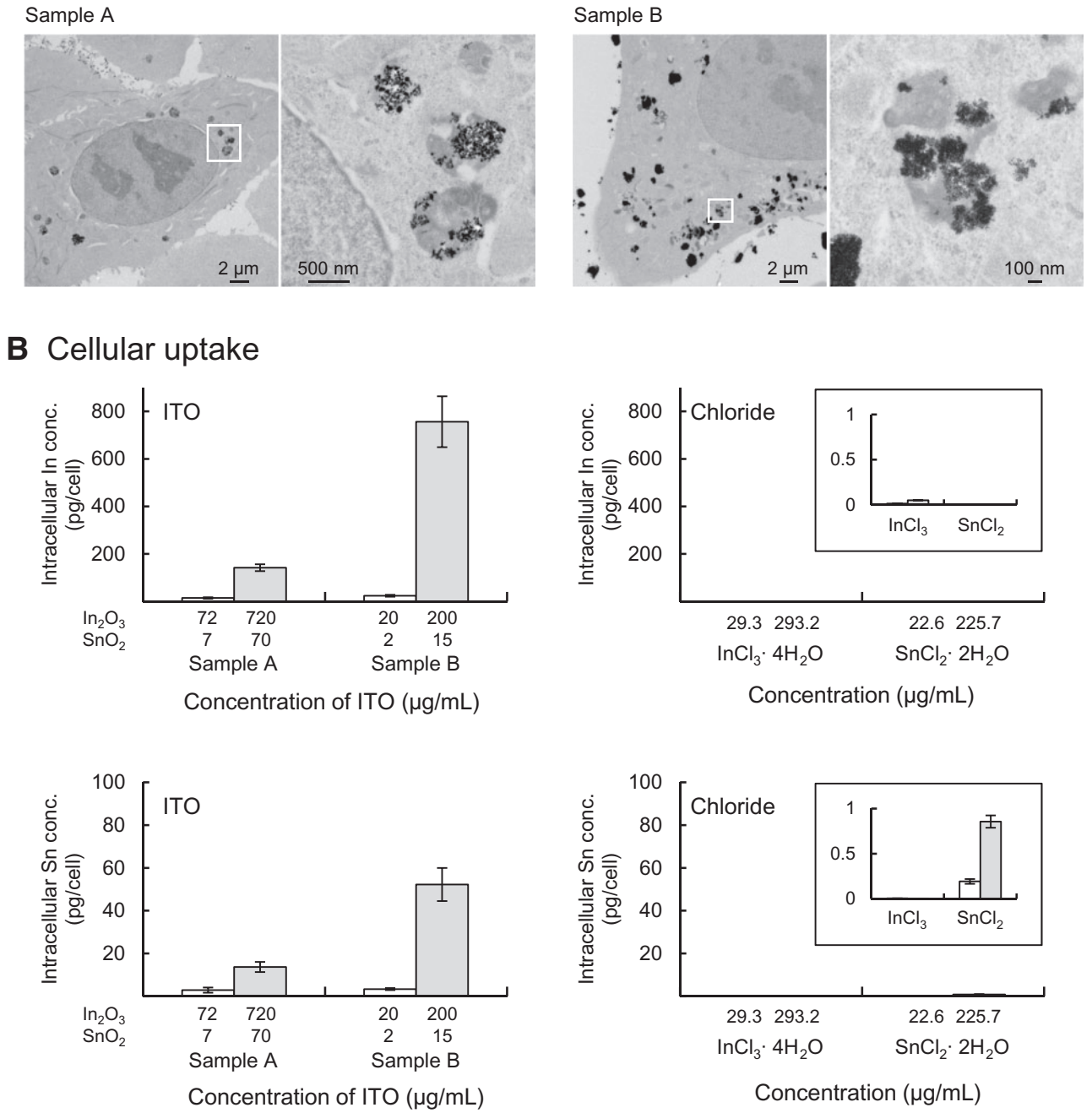

Fig. 2 Cellular uptake of ITO NPs by A549 cells. (**A**) TEM observation of A549 cells exposed to stable ITO dispersions for 24 h. Overview of the cell (left) and detail of the part in the white frame (right). The exposed concentrations of In_2O_3 in Sample A and Sample B were 720 and 200 μg/ml, respectively. (**B**) Internal concentrations of indium and tin obtained by ICP-MS measurement. The A549 cells were exposed to stable ITO dispersion, $InCl_3$ or $SnCl_2$ solutions for 24 h, and then intracellular concentrations of indium and tin were measured by ICP-MS. Inset figures depict the data for the low intracellular concentration of indium and tin (0–1.0 pg/cell).

nuclei and mitochondria, did not contain ITO NPs. Previous reports indicate that micro-scale ITO particles were not readily taken up by lung epithelial cells (*34*). This difference in results may be due to differences in ITO particle size. Size-dependent cellular uptake has been reported for gold and silica NPs (*35*, *36*). Therefore, our results demonstrate that, similar to other NPs, ITO NPs can be readily taken up by human lung epithelial cells due to their small size.

The amount of indium and tin in the ITO NP-, $InCl_3$- or $SnCl_2$-exposed A549 cells was quantified by ICP-MS (Fig. 2B). After exposing A549 cells for 24 h, the entire cell population was detached and analysed after lysis to determine the internalized indium and tin concentrations. A clear increase in the intracellular indium and tin concentration was observed in both Sample A and Sample B. The indium and tin concentrations in cells exposed to Sample B were significantly

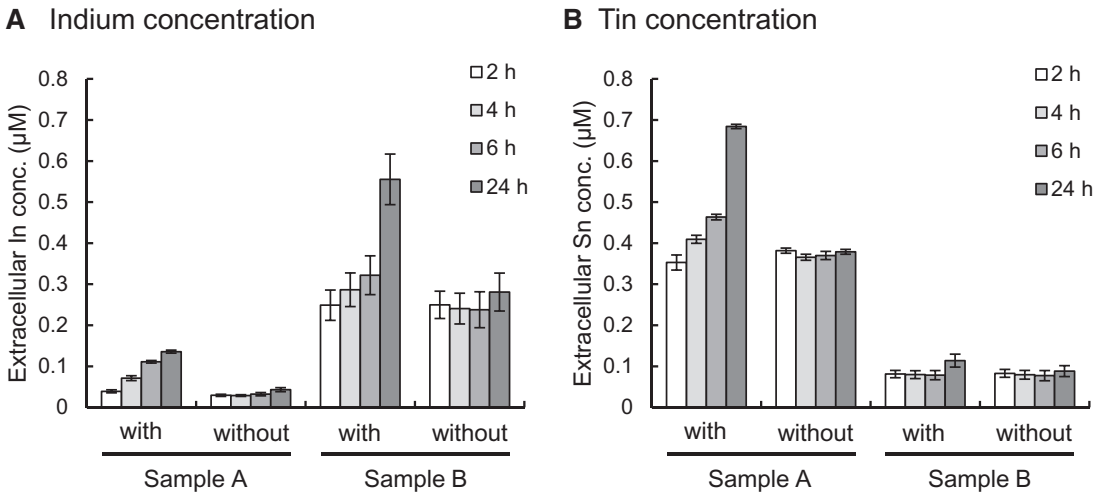

Fig. 3 Solubilization of ITO NPs within A549 cells. The stable ITO dispersions were incubated for 24 h with or without the A549 cells, and concentrations of (**A**) indium and (**B**) tin were measured in cell culture medium by ICP-MS. The exposed concentrations of In_2O_3 in Sample A and Sample B were 720 and 200 μg/ml, respectively.

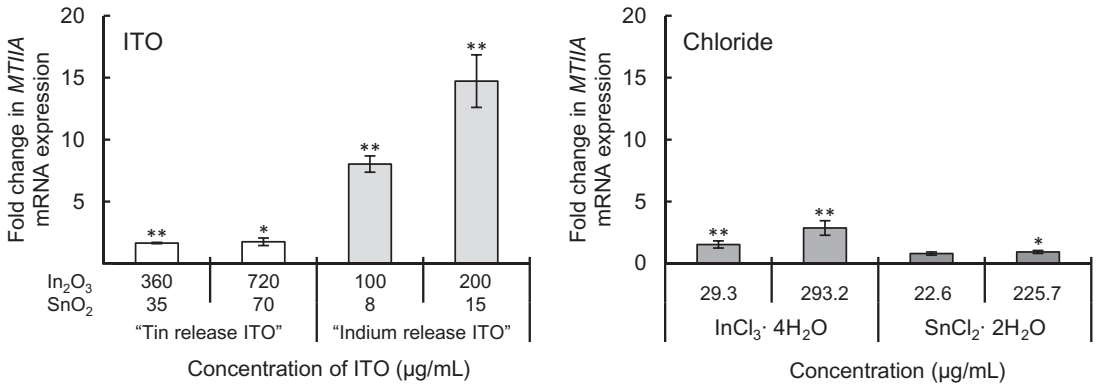

Fig. 4 The mRNA transcript levels of *MTIIA* in A549 cells exposed to stable ITO dispersions, $InCl_3$ or $SnCl_2$ solutions for 24 h. We measured the expression levels of *MTIIA* using real-time PCR. Each transcript level was normalized to corresponding *β-actin* values and were presented as relative units compared with untreated control. $*P<0.05$, $**P<0.01$ (versus control, Dunnett test, analysis of variance).

higher than that in cells exposed to Sample A. In contrast, $InCl_3$ and $SnCl_2$ were hardly incorporated into the A549 cells, as compared with ITO NPs. Our findings are consistent with the earlier reports on the increased cellular uptake of manganese oxide (Mn_3O_4), Ag and CuO NPs, as compared with soluble salts ($MnSO_4$, $AgNO_3$ and $CuCl_2$) (*12*, *37*). These results indicated that ITO NPs were readily incorporated into A549 cells, whereas their corresponding metal ions were not easily transported into cells.

Solubilization of ITO NPs within A549 cells

The solubilization of micro-scale ITO particles mediated by macrophages and epithelial cells was determined by measuring the extracellular release of indium ions (*38*). To determine whether the ITO NPs incorporated into A549 cells were solubilized, we measured extracellular release of ionic indium and tin at 2, 4, 6 and 24 h using ICP-MS (Fig. 3). As shown in Fig. 3, the concentration of total ionic indium in the medium from A549 cells treated with Sample B was higher than cells treated with Sample A (Fig. 3A). Conversely, the concentration of total ionic tin in the medium from A549 cells treated with Sample B was lower than cells treated with Sample A (Fig. 3B). In general, ITO is insoluble at physiological pH (*25*). Indeed, our results show that the solubilization of ITO NPs was not observed in the absence of A549 cells. Recently, Sabella *et al.* (*39*) demonstrated that a wide variety of NPs incorporated into cells were degraded, and released corresponding ions in the acidic environment of lysosomes. Additionally, Gwinn *et al.* (*38*) reported that micro-scale ITO particles taken up by macrophages were solubilized via phagolysosomal acidification. Our results show that intracellular ITO NPs localized in lysosome-like structures were dissolved, which resulted in the release of indium or tin ions by lysosomal acidification. Furthermore, we found that when the ITO NPs were solubilized within the A549 cells, the metal ions released from Sample A were primarily tin ions (hereafter referred to as 'tin release ITO'), whereas those released from Sample B were indium ions (hereafter referred to as 'indium release ITO').

Metallothionein IIA mRNA expression

Metallothioneins are low molecular weight, cysteine-rich metal-binding proteins found in a variety of

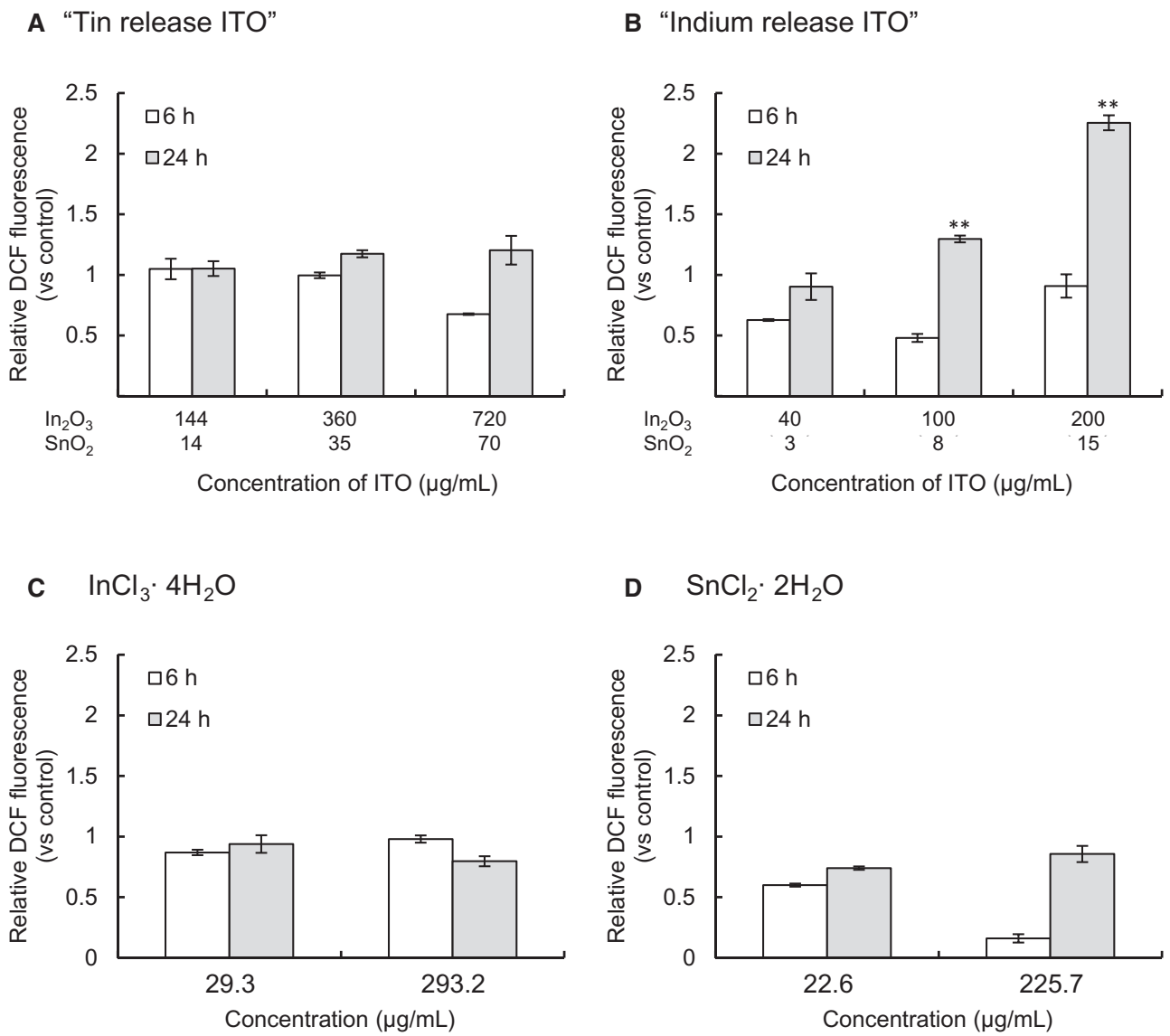

Fig. 5 Intracellular ROS levels in A549 cells exposed to stable ITO dispersion, $InCl_3$ or $SnCl_2$ solutions. Cells were exposed to stable ITO dispersions (**A**, **B**), $InCl_3$ (**C**) or $SnCl_2$ (**D**) for 6 or 24 h. Intracellular ROS levels were measured by the DCFH method using flow cytometry. The standardized DCF fluorescence value for untreated controls was 1. $^{**}P<0.01$ (versus control, Dunnett test, analysis of variance).

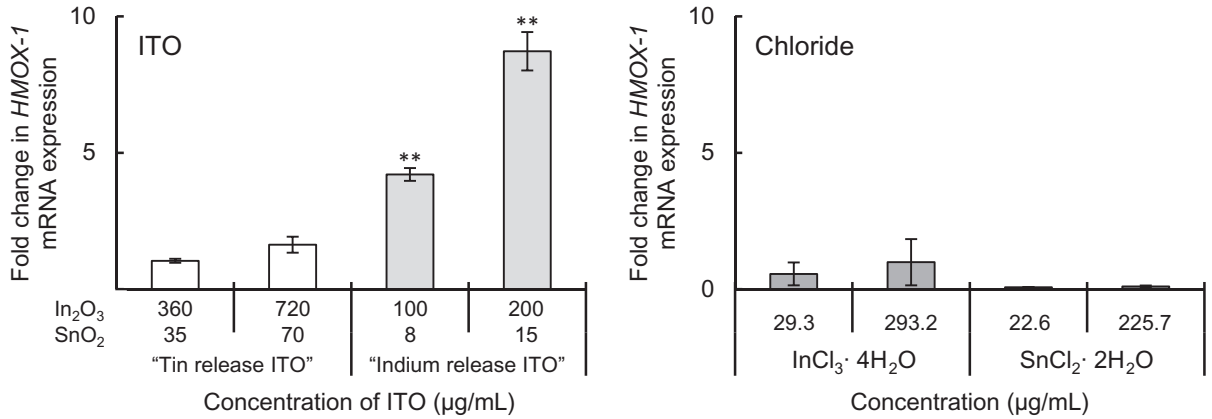

Fig. 6 The mRNA transcript levels of *HMOX-1* in A549 cells exposed to stable ITO dispersion, $InCl_3$ or $SnCl_2$ solutions. The expression level of *HMOX-1* was measured using real-time PCR. Each transcript level was normalized to the corresponding *β-actin* value, and presented as relative units compared with untreated control. $^{**}P<0.01$ (versus control, Dunnett test, analysis of variance).

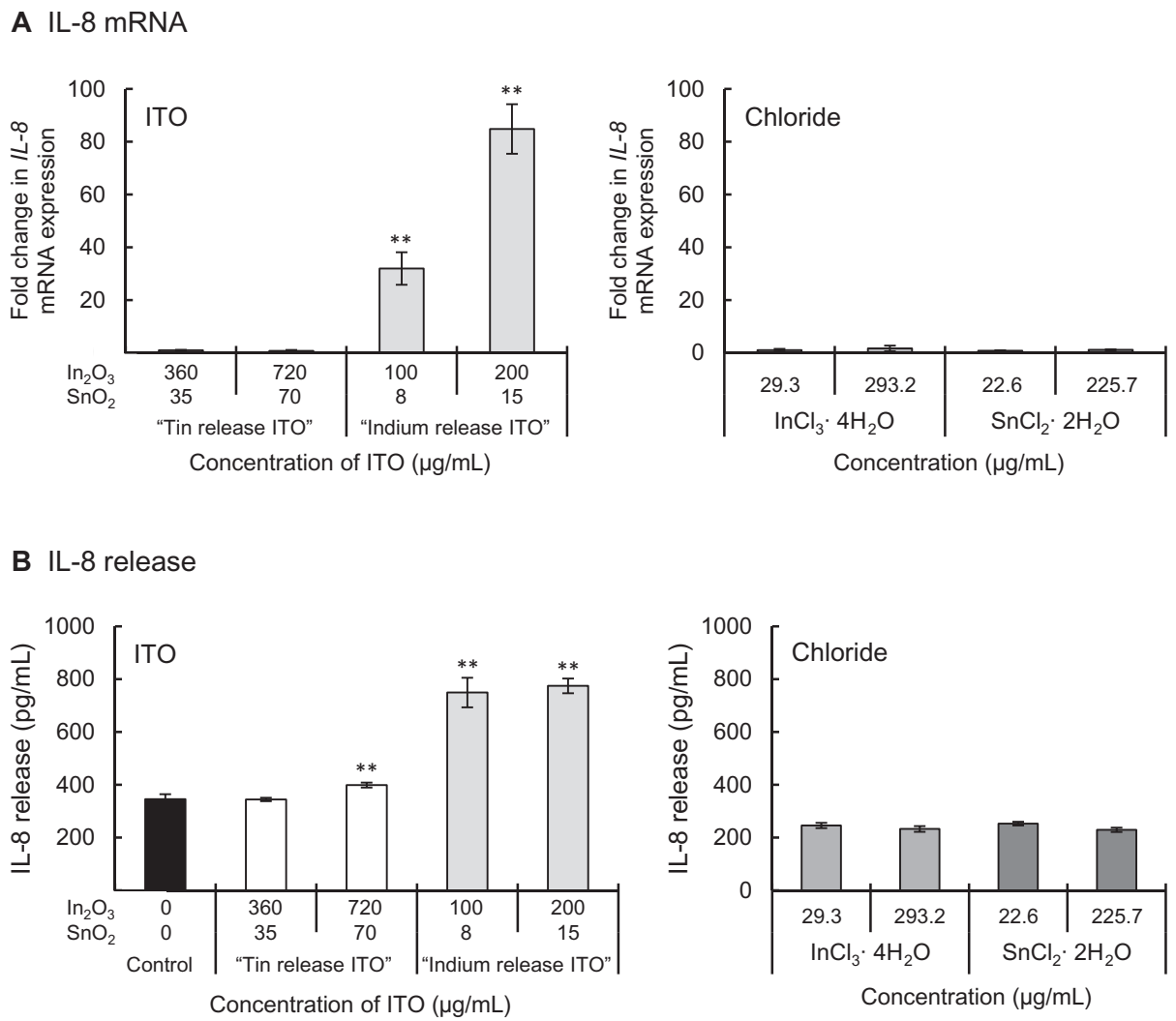

Fig. 7 The transcript levels and protein release of IL-8 in A549 cells exposed to stable ITO dispersion, $InCl_3$ or $SnCl_2$ solutions. We measured the expression level of *IL-8* using real-time PCR (**A**) and IL-8 release from A549 cells using enzyme-linked immunosorbent assay (**B**). Each transcript level was normalized to the corresponding *β-actin* value, and presented as relative units compared with untreated control. $^{**}P<0.01$ (versus control, Dunnett test, analysis of variance).

organisms, including bacteria, plants, invertebrates and vertebrates (*40*–*42*). Metallothioneins play a role in metal homeostasis and detoxification by controlling intracellular-free metal levels (*40*, *43*). The *MTIIA* gene, a widely distributed isoform, is expressed under basal condition and is induced by heavy metals (*44*). We analysed the expression of *MTIIA* mRNA in A549 cells exposed to stable ITO dispersions, $InCl_3$ or $SnCl_2$ solutions for 24 h (Fig. 4). The mRNA levels of *MTIIA* dose dependently increased after incubation with indium release ITO. The expression of *MTIIA* was also induced after incubation with tin release ITO, $InCl_3$ or $SnCl_2$; however, the induction levels were not remarkable. These results indicate that the expression of *MTIIA* is induced by intracellular accumulation of indium ions.

Effects of stable ITO dispersions on oxidative stress

Metallothioneins both regulate metal detoxification and protect against oxidative stress (*45*, *46*). Thus, we examined the effect of ITO NPs on oxidative stress. The stable ITO dispersion, $InCl_3$ or $SnCl_2$ solutions were exposed to A549 cells for 6 or 24 h, and intracellular ROS levels were measured using the fluorescence dye, DCFH-DA, which shows enhanced fluorescence during oxidative stress (Fig. 5). After exposure to indium release ITO for 24 h, we observed a significant increase in intracellular ROS production (Fig. 5B). In contrast, we did not detect a significant increase in intracellular ROS when cells were exposed to tin release ITO, $InCl_3$ or $SnCl_2$ solutions for 24 h (Fig. 5A, C and D).

We also measured the mRNA levels of *HMOX-1*, a marker of oxidative stress, to determine the response of A549 cells exposed to the stable ITO dispersions, $InCl_3$ or $SnCl_2$ solutions for 24 h (Fig. 6). The mRNA levels of *HMOX-1* were dose dependently increased after incubation with indium release ITO, consistent with ROS production. However, *HMOX-1* expression was not increased in cells exposed to tin release ITO, $InCl_3$ or $SnCl_2$ solutions. These results indicate that oxidative stress was induced by the accumulation of intracellular indium ions, but not by intracellular tin ion or extracellular indium or tin ions.

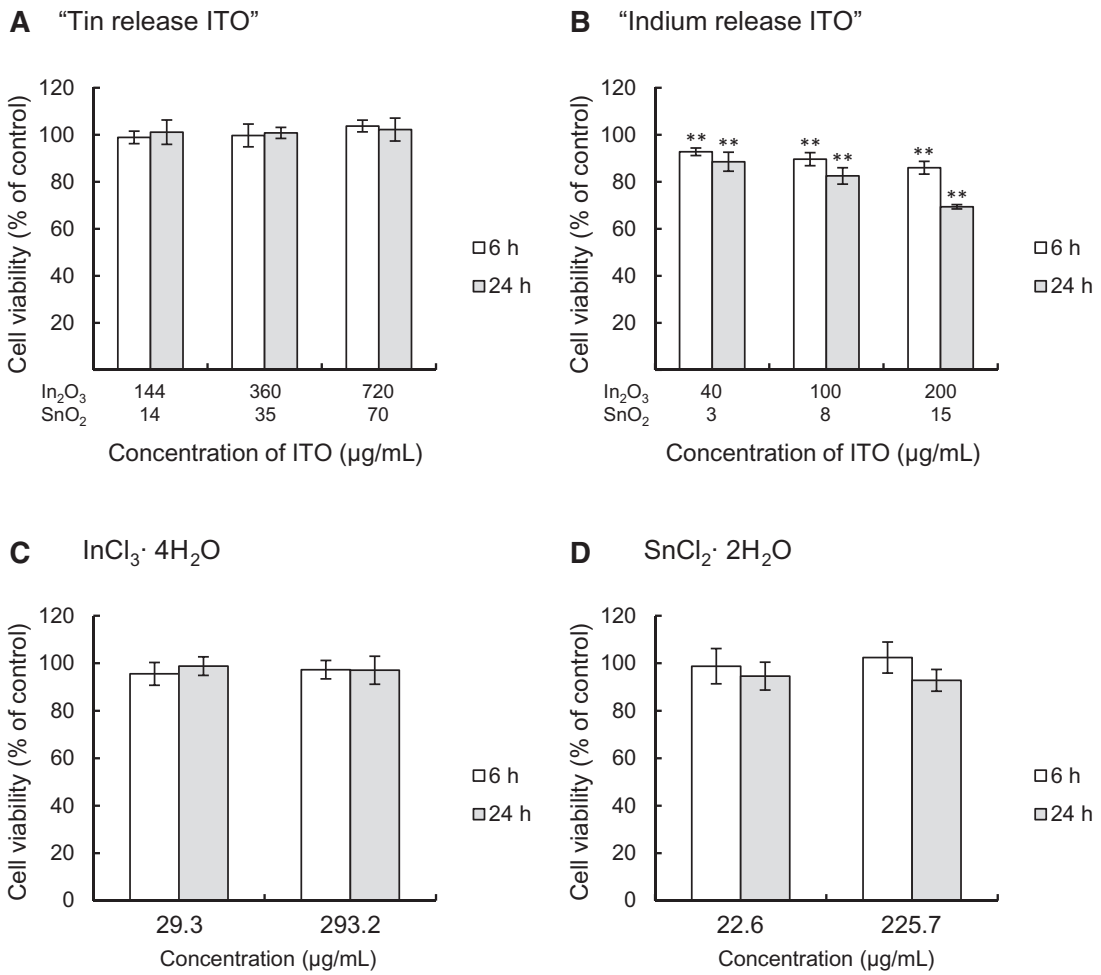

Fig. 8 Effect of stable ITO dispersion, $InCl_3$ or $SnCl_2$ solutions on cell viability. Cells were exposed to stable ITO dispersions (A and B), $InCl_3$ (C) or $SnCl_2$ (D) solutions for 6 or 24 h. The cell viability was measured using the WST-1 assay, and the results were given as percent of untreated controls. $^{**}P < 0.01$ (versus control, Dunnett test, analysis of variance).

IL-8 mRNA and protein expression

An increase in intracellular ROS generation can result in pro-inflammatory and cytotoxic effects (*47*, *48*). Lung epithelial cells are important source of IL-8, and IL-8 serves attracts neutrophils to the site of inflammation (*49*, *50*). Moreover, IL-8 is shown to be induced in A549 cells via a mechanism involving oxidative stress and the redox-sensitive transcription factor nuclear factor kappa-B (*51*, *52*). To investigate inflammatory responses in A549 cells, we examined the expression of *IL-8* mRNA in A549 cells exposed to stable ITO dispersions, $InCl_3$ or $SnCl_2$ solutions for 24 h (Fig. 7A). *IL-8* mRNA levels were significantly and dose-dependently induced in indium release ITO-exposed cells, whereas no effect was observed in tin release ITO-, $InCl_3$- or $SnCl_2$-treated cells. We also quantified IL-8 protein levels released into the cell culture medium at 24 h (Fig. 7B). Consistent with mRNA expression data, indium release ITO exposure increased IL-8 protein release from A549 cells 24 h after exposure. Taken together, these results indicate that indium release ITO exposure upregulated IL-8 expression at both the mRNA and protein level in A549 cells.

Effect of stable ITO dispersions on cell viability and membrane integrity

In a previous report, micro-scale ITO particles were not cytotoxic to lung-derived epithelial cells even at a high concentration level of 400 μg/ml (*38*). Then, the effect of ITO NPs, $InCl_3$ and $SnCl_2$ on cell viability was examined by WST-1 assay after 6- or 24-h treatment (Fig. 8). Cell viability decreased with increasing concentrations of indium release ITO (Fig. 8B). In contrast, no inhibition was observed using tin release ITO, $InCl_3$ or $SnCl_2$ (Fig. 8A, C and D). Furthermore, we measured the cell membrane integrity after incubation with stable ITO dispersions, $InCl_3$ or $SnCl_2$ solutions for 6 or 24 h (Fig. 9). No significant damage was observed after tin release ITO or $SnCl_2$ treatment (Fig. 9A and D). Indium release ITO did not have a remarkable effect on cell membranes, although membrane damage was observed after 24 h at the highest dose (Fig. 9B). We also found that exposure to high $InCl_3$ concentrations induced membrane damage in A549 cells (Fig. 9C). These results indicate that cell membrane damage is induced by extracellular indium ions, but not intracellular accumulation of indium ions.

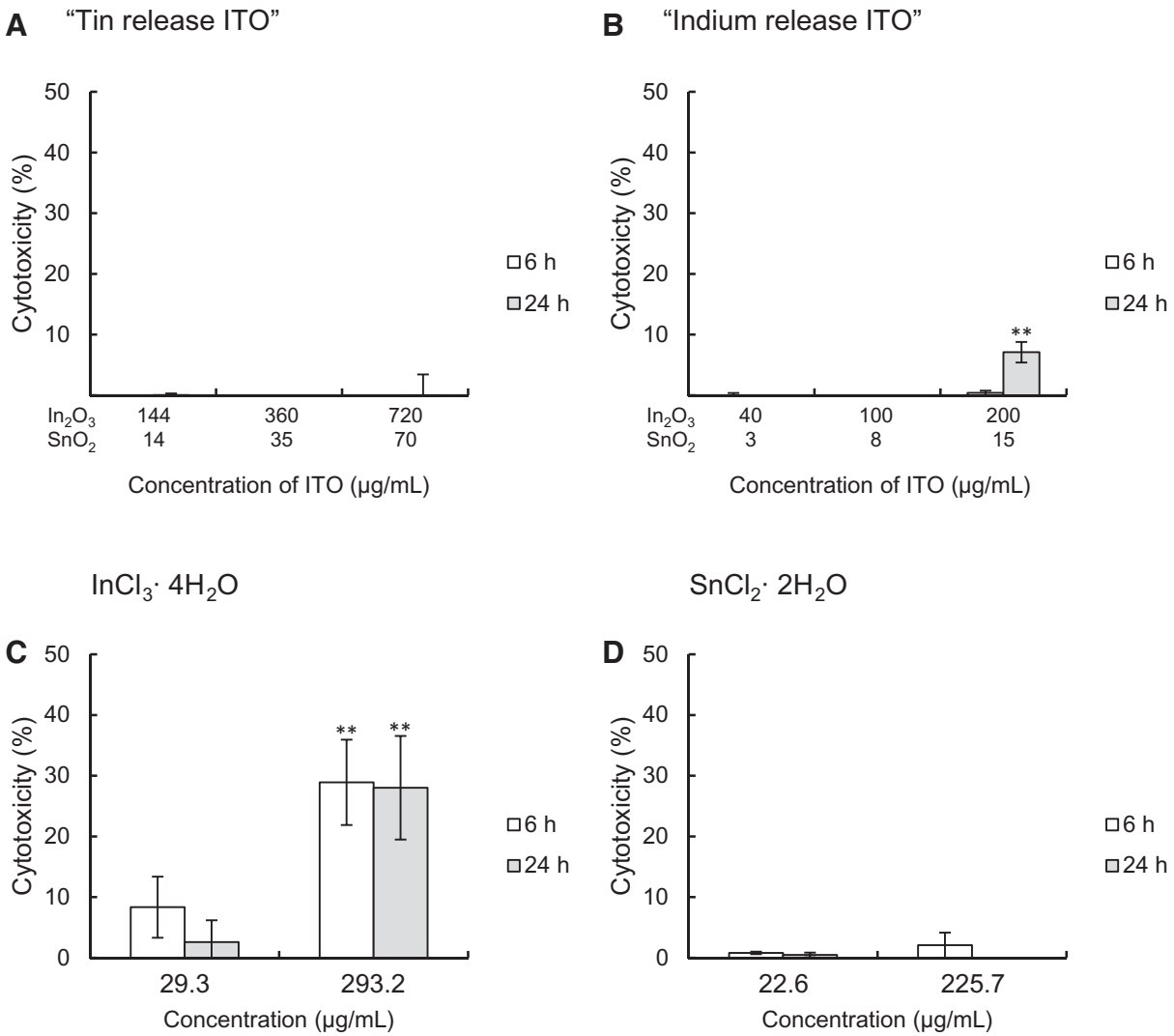

Fig. 9 Effect of stable ITO dispersions, $InCl_3$ or $SnCl_2$ solutions on the cell membrane. The cells were exposed to stable ITO dispersions (A and B), $InCl_3$ (C) or $SnCl_2$ (D) solutions for 6 or 24 h. Cell membrane damage was determined by measuring intracellular LDH release. The method of calculating cytotoxicity is described in the Experimental procedure section. $^{**}P<0.01$ (versus control, Dunnett test, analysis of variance).

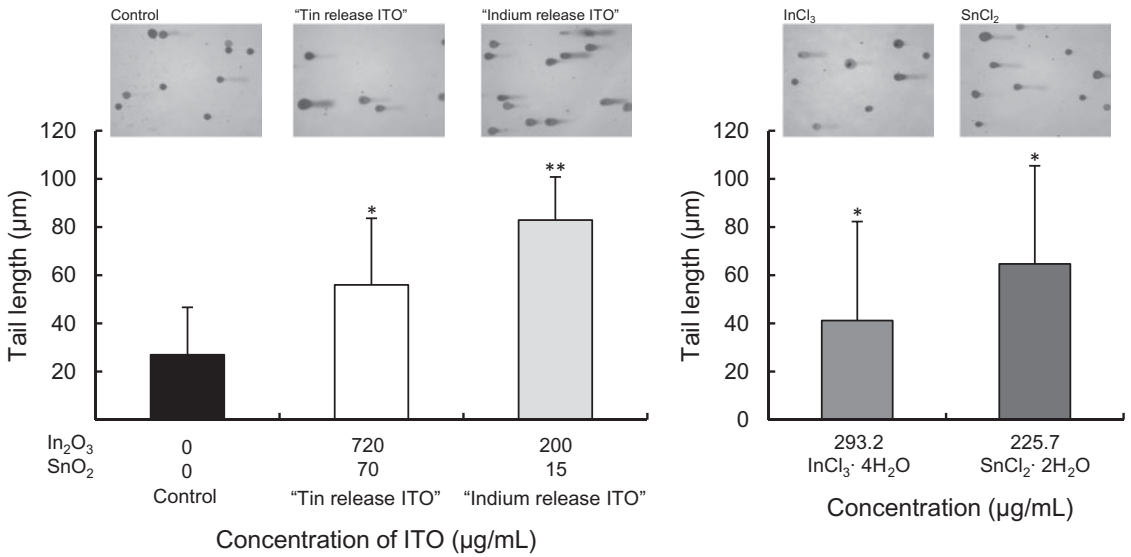

Fig. 10 Effect of stable ITO dispersions, $InCl_3$ or $SnCl_2$ solutions on DNA integrity. A549 cells were exposed to stable ITO dispersions, $InCl_3$ or $SnCl_2$ solutions for 24 h. The DNA tail length values were obtained by analysing at least 50 random comet images from each treatment. The upper pictures are comet images of untreated (control), ITO NPs, $InCl_3$ and $SnCl_2$-exposed cells. $^{*}P<0.05$, $^{**}P<0.01$ (versus control, Dunnett test, analysis of variance).

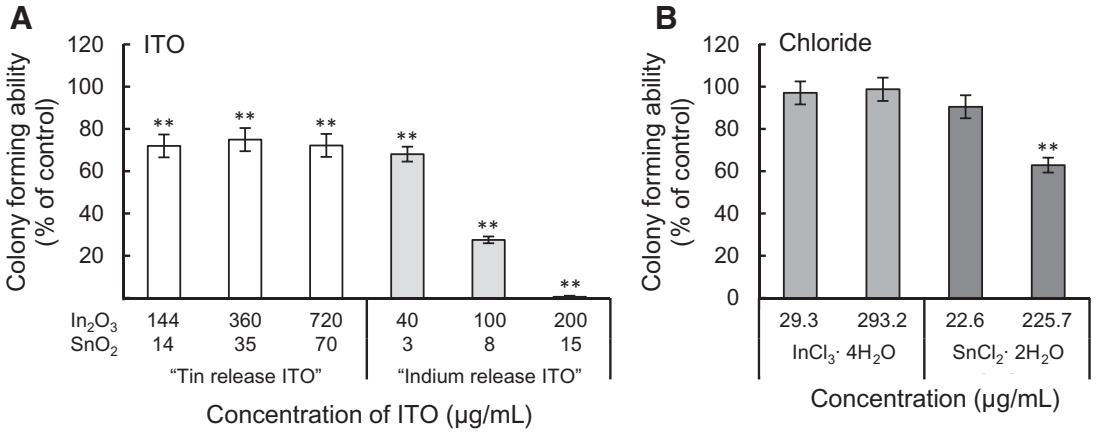

Fig. 11 Clonogenic assays in cells exposed to stable ITO dispersions, $InCl_3$ or $SnCl_2$ solutions. After the cells were cultured with the stable ITO dispersions, $InCl_3$ or $SnCl_2$ solutions for 7 days, the number of colonies were counted. Colony-forming ability was standardized to the untreated cells (100%). $^{**}P<0.01$ (versus control, Dunnett test, analysis of variance).

DNA damage and colony-forming ability in A549 cells

Several studies indicated that oxidative stress induces a wide variety of physiological and cellular effects, including DNA damage (*53*). Thus, we examined DNA single-strand breaks using alkaline comet assays. A549 cells were incubated with the stable ITO dispersions, $InCl_3$ or $SnCl_2$ solutions for 24 h. Representative DNA damage images are shown in Fig. 10. The ITO NPs induced DNA strand breakage over 24 h; however, only a slight difference was observed between the indium release ITO and tin release ITO. The comet tail lengths of the indium release ITO-exposed cells were longer than that of the tin release ITO-exposed cells. We also found that exposure to $InCl_3$ and $SnCl_2$ induced DNA damage, with $SnCl_2$ having a greater effect. However, the DNA damage results were not correlated with intracellular ROS levels. Previous reports indicated that DNA repair enzyme activity was inhibited by exposure to indium (*54*). Additionally, it was suggested that tin ions have DNA damage potential via direct interactions with DNA (*55*). Therefore, DNA damage induced by ITO NPs is mediated by increased oxidative stress, inhibition of DNA repair enzymes and direct interaction of indium and/or tin ions with DNA.

The influence of ITO NPs, $InCl_3$ and $SnCl_2$ on colony-forming ability was examined using a clonogenic assay (Fig. 11). The clonogenic assay revealed that indium release ITO dose dependently inhibited colony formation. Incubation with tin release ITO induced a statistically significant, but not a dose dependent, inhibition of colony formation. No inhibition was observed using $InCl_3$ and $SnCl_2$, although $SnCl_2$ slightly inhibited colony formation at the highest concentration. These results suggest that the accumulation of intracellular indium ions induced the loss of DNA integrity and loss of colony-forming ability.

The present *in vitro* data suggest that cellular effects induced by the exposure of indium release ITO might be caused by cellular uptake of a higher number of NPs and subsequent release of indium ions. Evaluating the cellular responses, other cell types including type I and II alveolar epithelial cells and alveolar macrophages would further contribute to our understanding of the mechanisms of ITO-related lung diseases. Furthermore, future studies would be important to establish if the present studies obtained from the A549 cells also apply to the *in vivo* environment.

Conclusion

In this study, we investigated the effect of two types of ITO NPs, indium release ITO and tin release ITO, on human lung epithelial cells. We found that indium release ITO, but not tin release ITO, has significant cellular effects. The NPs enable high uptake and intracellular solubilization leading to high levels of intracellular indium ionic species following cell exposure to indium release ITO. In contrast, a high uptake but few cellular effects were observed using tin release ITO, most likely due to low intracellular release of indium ions. Thus, controlling metal ion release from ITO NPs enables us to minimize and reduce NP-associated health risks, and avoid unnecessary prohibition of beneficial NPs. To our knowledge, this is the first report that describes the relationship between cellular effects and intracellular ITO NP solubility. The cellular effects induced by exposures to ITO NPs may provide insights into indium-mediated lung disease.

Acknowledgements

The authors are thankful to Ms Emiko Kobayashi, Bioproduction Research Institute, National Institute of Advanced Industrial Science and Technology for carrying out the transmission electron microscopy.

Conflict of Interest
None declared.

References

1. Oberdörster, G., Oberdörster, E., and Oberdörster, J. (2005) Nanotoxicology: an emerging discipline evolving from studies of ultrafine particles. *Environ. Health Perspect*. **113**, 823–839

2. De Jong, W.H. and Borm, P.J. (2008) Drug delivery and nanoparticles: application and hazards. *Int. J. Nanomedicine* **3**, 133–149
3. Doane, T.L. and Burda, C. (2012) The unique role of nanoparticles in nanomedicine: imaging, drug delivery and therapy. *Chem. Soc. Rev.* **41**, 2885–2911
4. Song, W., Zhang, J., Guo, J., Zhang, J., Ding, F., Li, L., and Sun, Z. (2010) Role of the dissolved zinc ion and reactive oxygen species in cytotoxicity of ZnO nanoparticles. *Toxicol. Lett.* **199**, 389–397
5. Huang, C.C., Aronstam, R.S., Chen, D.R., and Huang, Y.W. (2010) Oxidative stress, calcium homeostasis, and altered gene expression in human lung epithelial cells exposed to ZnO nanoparticles. *Toxicol. In Vitro* **24**, 45–55
6. Heng, B.C., Zhao, X., Tan, E.C., Khamis, N., Assodani, A., Xiong, S., Ruedl, C., Ng, K.W., and Loo, J.S. (2011) Evaluation of the cytotoxicity and inflammatory potential of differentially shaped zinc oxide nanoparticles. *Arch. Toxicol.* **85**, 1517–1528
7. Fukui, H., Horie, M., Endoh, S., Kato, H., Fujita, K., Nishio, K., Komaba, L.K., Maru, J., Miyauchi, A., Nakamura, A., Kinugasa, S., Yoshida, Y., Hagihara, Y., and Iwahashi, H. (2012) Association of zinc ion release and oxidative stress induced by intratracheal instillation of ZnO nanoparticles to rat lung. *Chem. Biol. Interact.* **198**, 29–37
8. Horie, M., Fujita, K., Kato, H., Endoh, S., Nishio, K., Komaba, L.K., Nakamura, A., Miyauchi, A., Kinugasa, S., Hagihara, Y., Niki, E., Yoshida, Y., and Iwahashi, H. (2012) Association of the physical and chemical properties and the cytotoxicity of metal oxide nanoparticles: metal ion release, adsorption ability and specific surface area. *Metallomics* **4**, 350–360
9. Brunner, T.J., Wick, P., Manse, P., Spohn, P., Grass, R.N., Limbach, L.K., Bruinink, A., and Stark, W.J. (2006) *In vitro* cytotoxicity of oxide nanoparticles: comparison to asbestos, silica, and the effect of particle solubility. *Environ. Sci. Technol.* **40**, 4374–4381
10. Horie, M., Nishio, K., Fujita, K., Kato, H., Nakamura, A., Kinugasa, S., Endoh, S., Miyauchi, A., Yamamoto, K., Murayama, H., Niki, E., Iwahashi, H., Yoshida, Y., and Nakanishi, J. (2009) Ultrafine NiO particles induce cytotoxicity *in vitro* by cellular uptake and subsequent Ni(II) release. *Chem. Res. Toxicol.* **222**, 1415–1426
11. Horie, M., Nishio, K., Endoh, S., Kato, H., Fujita, K., Miyauchi, A., Nakamura, A., Kinugasa, S., Yamamoto, K., Niki, E., Yoshida, Y., and Iwahashi, H. (2013) Chromium(III) oxide nanoparticles induced remarkable oxidative stress and apoptosis on culture cells. *Environ. Toxicol.* **28**, 61–75
12. Cronholm, P., Karlsson, H.L., Hedberg, J., Lowe, T.A., Winnberg, L., Elihn, K., Wallinder, I.O., and Möller, L. (2013) Intracellular uptake and toxicity of Ag and CuO nanoparticles: a comparison between nanoparticles and their corresponding metal ions. *Small* **9**, 970–982
13. Gliga, A.R., Skoglund, S., Wallinder, I.O., Fadeel, B., and Karlsson, H.L. (2014) Size-dependent cytotoxicity of silver nanoparticles in human lung cells: the role of cellular uptake, agglomeration and Ag release. *Part. Fibre Toxicol.* **11**, 11
14. Betz, U., Kharrazi Olsson, M., Marthy, J., Escolá, M.F., and Atamny, F. (2006) Thin film engineering of indium tin oxide: large area flat panel displays application. *Surf. Coat. Technol.* **200**, 5751–5759
15. Fthenakis, V. (2009) Sustainability of photovoltaics: the case for thin-film solar cells. *Renew. Sustain. Energy Rev.* **13**, 2746–2750
16. Ng, H.T., Fang, A.P., Huang, L.Q., and Li, S.F.Y. (2002) Protein microarray on ITO surfaces by a direct covalent attachment scheme. *Langmuir* **18**, 6324–6329
17. McCue, J.T. and Ying, J.Y. (2009) SnO_2-In_2O_3 nanocomposites as semiconductor gas sensors for CO and NO_x detection. *Chem. Mater.* **19**, 1009–1015
18. Kim, K.Y. and Park, S.B. (2004) Preparation and property control of nano-sized indium tin oxide particle. *Mater. Chem. Phys.* **86**, 210–221
19. Song, J.E., Lee, D.K., Kim, H.W., Kim, Y.I., and Kang, Y.S. (2005) Preparation and characterization of monodispersed indium-tin oxide nanoparticles. *Colloids Surf. A Physicochem. Eng. Asp.* **257–258**, 539–542
20. Takagi, R., Suzuki, Y., Seki, Y., Ikehata, M., Kajihara, C., Shimizu, H., and Yanagisawa, H. (2011) Indium chloride-induced micronuclei in *in vivo* and *in vitro* experimental system. *J. Occup. Health* **53**, 102–109
21. Viau, C.M., Guecheva, T.N., Sousa, F.G., Pungartnik, C., Brendel, M., Saffi, J., and Henriques, J.A. (2009) $SnCl_2$-induced DNA damage and repair inhibition of MMS-caused lesions in V79 Chinese hamster fibroblasts. *Arch. Toxicol.* **83**, 769–775
22. Badding, M.A., Schwegler-Berry, D., Park, J.H., Fix, N.R., Cummings, K.J., and Leonard, S.S. (2015) Sintered indium-tin oxide particles induce pro-inflammatory responses *in vitro*, in part through inflammasome activation. *PLoS One* **10**, e0124368
23. Homma, T., Ueno, T., Sekizawa, K., Tanaka, A., and Hirata, M. (2003) Interstitial pneumonia developed in a worker dealing with particles containing indium-tin oxide. *J. Occup. Health* **45**, 137–139
24. Chonan, T., Taguchi, O., and Omae, K. (2007) Interstitial pulmonary disorders in indium-processing workers. *Eur. Respir. J.* **29**, 317–324
25. Hamaguchi, T., Omae, K., Takebayashi, T., Kikuchi, Y., Yoshioka, N., Nishiwaki, Y., Tanaka, A., Hirata, M., Taguchi, O., and Chonan, T. (2008) Exposure to hardly soluble indium compounds in ITO production and recycling plants is a new risk for interstitial lung damage. *Occup. Environ. Med.* **65**, 51–55
26. Nakano, M., Omae, K., Tanaka, A., Hirata, M., Michikawa, T., Kikuchi, Y., Yoshioka, N., Nishiwaki, Y., and Chonan, T. (2009) Causal relationship between indium compound inhalation and effects on the lungs. *J. Occup. Health* **51**, 513–521
27. Cummings, K.J., Donat, W.E., Ettensohn, D.B., Roggli, V.L., Ingram, P., and Kreiss, K. (2010) Pulmonary alveolar proteinosis in workers at an indium processing facility. *Am. J. Respir. Crit. Care Med.* **181**, 458–464
28. Tabei, Y., Sonoda, A., Nakajima, Y., Biju, V., Makita, Y., Yoshida, Y., and Horie, M. (2015) *In vitro* evaluation of the cellular effect of indium tin oxide nanoparticles using the human lung adenocarcinoma A549 cells. *Metallomics* **7**, 816–827
29. Herzog, E., Casey, A., Lyng, F.M., Chambers, G., Byrne, H.J., and Davoren, M. (2007) A new approach to the toxicity testing of carbon-based nanomaterilals—the clonogenic assay. *Toxicol. Lett.* **174**, 49–60
30. Franken, N.A., Rodermond, H.M., Stap, J., Haveman, J., and van Bree, C. (2006) Clonogenic assay of cells *in vitro*. *Nat. Protoc.* **1**, 2315–2319
31. Horie, M., Kato, H., Fujita, K., Endoh, S., and Iwahashi, H. (2012) *In vitro* evaluation of cellular

response induced by manufactured nanoparticles. *Chem. Res. Toxicol.* **25**, 605–619

32. Teeguarden, J.G., Hinderliter, P.M., Orr, G., Thrall, B.D., and Pounds, J.G. (2007) Particokinetics *in vitro*: dosimetry considerations for *in vitro* nanoparticle toxicity assessments. *Toxicol. Sci.* **95**, 300–312
33. Kato, H., Suzuki, M., Fujita, K., Horie, M., Endoh, S., Yoshida, Y., Iwahashi, H., Takahashi, K., Nakamura, A., and Kinugasa, S. (2009) Reliable size determination of nanoparticles using dynamic light scattering method for *in vitro* toxicity assessment. *Toxicol. In Vitro* **23**, 927–934
34. Lison, D., Laloy, J., Corazzari, I., Muller, J., Rabolli, V., Panin, N., Huaux, F., Fenoglio, I., and Fubini, B. (2009) Sintered indium-tin-oxide (ITO) particles: a new pneumotoxic entry. *Toxicol. Sci.* **108**, 472–481
35. Jiang, W., Kim, B.Y., Rutka, J.T., and Chan, W.C. (2008) Nanoparticle-mediated cellular response is size-dependent. *Nat. Nanotechnol.* **3**, 145–150
36. Lu, F., Wu, S.H., Hung, Y., and Mou, C.Y. (2009) Size effect on cell uptake in well-suspended, uniform mesoporous silica nanoparticles. *Small* **5**, 1408–1413
37. Frick, R., Müller-Edenborn, B., Schlicker, A., Rothen-Rutishauser, B., Raemy, D.O., Günther, D., Hattendorf, B., Stark, W., and Beck-Schimmer, B. (2011) Comparison of manganese oxide nanoparticles and manganese sulfate with regard to oxidative stress, uptake and apoptosis in alveolar epithelial cells. *Toxicol. Lett.* **205**, 163–172
38. Gwinn, W.M., Qu, W., Shines, C.J., Bousquet, R.W., Taylor, G.J., Waalkes, M.P., and Morgan, D.L. (2013) Macrophage solubilization and cytotoxicity of indium-containing particles *in vitro*. *Toxicol. Sci.* **135**, 414–424
39. Sabella, S., Carney, R.P., Brunetti, V., Malvindi, M.A., Al-Juffali, N., Vecchio, G., Janes, S.M., Bakr, O.M., Cingolani, R., Stellacci, F., and Pompa, P.P. (2014) A general mechanism for intracellular toxicity of metal-containing nanoparticles. *Nanoscale* **6**, 7052–7061
40. Coyle, P., Philcox, J.C., Carey, L.C., and Rofe, A.M. (2002) Metallothionein: the multipurpose protein. *Cell. Mol. Life Sci.* **59**, 627–647
41. Henkel, G. and Krebs, B. (2004) Zinc, cadmium, mercury, and copper thiolates and selenolates mimicking protein active site features—structural aspects and biological implications. *Chem. Rev.* **104**, 801–824
42. Vasák, M. (2005) Advances in metallothionein structure and functions. *J. Trace Elem. Med. Biol.* **19**, 13–17
43. Cherian, M.G., Jayasurya, A., and Bay, B.H. (2003) Metallothioneins in human tumors and potential roles in carcinogenesis. *Mutat. Res.* **533**, 201–209
44. Palmiter, R.D. (1994) Regulation of metallothionein genes by heavy metal appears to be mediated by a zinc-sensitive inhibitor that interacts with a constitutively active transcription factor, MTF-1. *Proc. Natl. Acad. Sci. U.S.A.* **91**, 1219–1223
45. Colangelo, D., Mahboobi, H., Viarengo, A., and Osella, D. (2004) Protective effect of metallothioneins against oxidative stress evaluated on wild type and MT-null cell lines by means of flow cytometry. *BioMetals* **17**, 365–370
46. Klaassen, C.D., Liu, J., and Diwan, B.A. (2009) Metallothionein protection of cadmium toxicity. *Toxicol. Appl. Pharmacol.* **238**, 215–220
47. Xiao, G.G., Wang, M., Li, N., Loo, J.A., and Nel, A.E. (2003) Use of proteomics to demonstrate a hierarchical oxidative stress response to diesel exhaust particle chemicals in a macrophage cell line. *J. Biol. Chem.* **278**, 50781–50790
48. Nel, A., Xia, T., Madler, L., and Li, N. (2006) Toxic potential of materials at the nanolevel. *Science* **311**, 622–627
49. Kunkel, S.L., Standiford, T., Kasahara, K., and Strieter, R.M. (1991) Interleukin-8 (IL-8): the major neutrophil chemotactic factor in the lung. *Exp. Lung Res.* **17**, 17–23
50. Sayes, C.M., Wahi, R., Kurian, P.A., Liu, Y., West, J.L., Ausman, K.D., Warheit, D.B., and Colvin, V.L. (2006) Correlating nanoscale titania structure with toxicity: a cytotoxicity and inflammatory response study with human dermal fibroblasts and human lung epithelial cells. *Toxicol. Sci.* **92**, 174–185
51. Kunsch, C. and Rosen, C.A. (1993) NF-kappa B subunit-specific regulation of the interleukin-8 promoter. *Mol. Cell. Biol.* **13**, 6137–6146
52. Schins, R.P.F. and Donaldson, K. (2000) Nuclear factor kappa-B activation by particle and fibers. *Inhal. Toxicol.* **12**, 317–326
53. AshaRani, P.V., Low Kah Mun, G., Hande, M.P., and Valiyaveettil, S. (2009) Cytotoxicity and genotoxicity of silver nanoparticles in human cells. *ACS Nano* **3**, 279–290
54. Bustamante, J., Dock, L., Vahter, M., Flowler, B., and Orrenius, S. (1997) The semiconductor elements arsenic and indium induce apoptosis in rat thymocytes. *Toxicology* **118**, 129–136
55. de Mattos, J.C., Dantas, F.J., Bezerra, R.J., Bernardo-Filho, M., Cabral-Neto, J.B., Lage, C., Leitão, A.C., and Caldeira-de-Araújo, A. (2000) Damage induced by stannous chloride in plasmid DNA. *Toxicol. Lett.* **116**, 159–163